ARCHIVES
of
FOUNDRY ENGINEERING
10.24425/afe.2025.155386
Published quarterly as the organ of the Foundry Commission of the Polish Academy of Sciences
ISSN (2299-2944)
Volume 2025
Issue 4/2025
103 – 108
14/4

Microstructure of Aluminium-TiC Composite Manufactured by Centrifugal Casting

S. Sobula *, T. Wiktor
AGH University of Krakow, Faculty of Foundry Engineering
al. A. Mickiewicza 30, 30-059 Krakow, Poland
* Corresponding author: E-mail address: sobula@agh.edu.pl

Received 23.05.25; accepted in revised form 18.07.25; available online 31.12.2025

Abstract

A numerical simulation of the casting of a metal matrix composite consisting of aluminium and TiC reinforcement was carried out using ProCAST software. To verify the results of the virtual experiment, a disc-shaped centrifugal composite casting was produced. The charge material consisted of Al/TiC metal matrix cast-composite scrap previously fabricated via the in situ self-propagating high-temperature synthesis in bath (SHS-B) method. This charge was remelted in an electric induction furnace and then poured into a vertically rotating mould made of furan sand. Microstructural examinations were carried out along the radius of the cast disc (150 mm in diameter) using scanning electron microscopy (SEM) and light microscopy (LM). The results demonstrated a gradual increase in both the material hardness and the volume fraction of the reinforced particles with increasing distance from the axis of rotation. In the outer region of the casting, the volume fraction of the reinforcing particles was approximately 50% higher compared to the region near the rotational axis. The results of the numerical simulation were in partial agreement with those obtained in a real experiment.

Keywords: Centrifugal casting, Functionally Graded Material, Aluminium matrix composite, TiC, Particle strengthening

1. Introduction

Typical functionally graded materials (FGMs) can be produced using various techniques, including infiltration of gradient spatial structure, additive manufacturing, sintering of gradient stacked powders and subsequent mould filling with melts of differing composition [1, 2]. In casting practice, bulk FGMs can be fabricated through direct solidification, centrifugal casting [3], sedimentation methods [4] and other techniques [2]. Reinforcing particles such as Al_2O_3, SiC, B_4C, and ZrO_2 are widely used to improve the strength of aluminium alloys [5].

Jackowski et al. [6] observed non-uniform distribution of SiC particles in the microstructure of the Al-SiC composite casting of turbine blades obtained by the centrifugal casting method. They conclude that the composite suspension fills equally the cavity of the turbine rotor mould with a thin wall, and the volume fraction of the particle was higher than that of the charge material.

Dolata et al. [7] examined the AlSi12 alloy with SiC and Al_2O_3 particles of different diameter. They showed that the composite containing a 10% volume fraction of reinforcing particles with diameters of 30, 50 and 100 μm exhibited a layered structure. The outer layer was predominantly composed of a larger Al_2O_3 particles (50-100 μm) while the inner layer contained smaller particles, primarily around 30 μm in size. Wang et al. [8] confirmed these observations in an experiment in which the Al - SiC slurry was centrifugally casted into the steel mould rotated with an angular speed of 800 rpm.

Carbides of transition metals like Ti, W, V, Nb and other were primarily used in iron alloys engineering to improve their wear resistance [9, 10, 11]. Nowadays, the use of titanium carbides represents a new approach to strengthening of aluminium alloys, particularly in materials developed for wear-resistant applications [12]. David Raja Selvam et al. [13] reported that the introduction of titanium carbide into the aluminium alloy in the amount of 2.5-10 vol. % improves the wear resistance of the A6061 alloy. Furthermore, the presence of TiC particles leads to the refinement of the microstructure in the examined alloy.

It is known that TiC is thermodynamically unstable in liquid aluminium, particularly within the temperature range of 700 - 800 °C. Prolonged holding of aluminium-TiC composites at these temperatures, promotes partial dissolution of TiC followed by precipitation of phases as Al_3Ti and Al_4C_3 [14].

Computer modelling of centrifugal casting of composites reinforced with solid particles can be a useful method for designing FGMs. Despite the difficulties in describing the thermal, physical, and chemical processes that occur during the pouring, flow, and solidification of particle suspensions, and this topic continues to be investigated by many researchers, [12, 15].

Verma et al. [11] simulated the flow behaviour of Al 6061 alloy containing 10% B_4C particles during horizontal centrifugal casting. They implemented a three-dimensional fluid dynamics model using Ansys Fluent software. Their model was based on the multiphase volume of fluid method and accounted for particle transport and alloy solidification. Furthermore, they assumed that mixture of the aluminium alloy and particles behaves as a Newtonian fluid, and that the B_4C particles are too small to consider them as separate phases and act as fluids. They obtained good agreement between the volume fraction of the particles in the cross sections of the examined wall in a real experiment and the computational simulation.

The phenomena of local density increasing and viscosity increasing in particle-rich layer have a significant influence on the simulation results. To solve this issue, Dolata et al. [16] examined the Eulerian model for prediction of particle arrangement in vertical-casted hollow cylinder. In this mathematical model, the slurry consisting of a metal alloy and particles is considered as a continuous phase, rather than a liquid with separate particles randomly distributed within it.

In our experiment, the ProCAST software was applied to simulate centrifugal casting of an aluminium matrix composite consisting of 10% vol. TiC reinforcement. Based on data acquired during a real examination, we attempted to replicate the experiment in a virtual environment. The ProCAST software does not have a dedicated module for simulating particle-containing alloys such as particle composites. To visualize the particle distribution in a centrifugal casting, we utilised the "Inclusion Particle Tracking" function in the post-processor.

2. Experiment

The main aim of our experiment was the fabrication of a functionally graded material composed of aluminium and titanium carbide particles (AFGM). The study consisted of two stages: a numerical simulation and a laboratory experiment. To implement the underlaying assumptions, a numerical study was first carried out, which confirmed the possibility of producing a casting with a gradient microstructure. In the simulation, the process was simplified by assuming that the reinforcing particles were introduced simultaneously with the liquid alloy into the pouring basin. Calculations were performed for particles of varying shapes, densities, and diameters.

An assumption for numerical experiment was as follows:

– the pouring temperature was adjusted to 710 °C;
– the viscosity of the alloy is equal to $1.12\cdot10^{-3}$ Pa·s, and the alloy density was 2.38 g/cm^3 at the pouring temperature;
– particle diameters were 20 and 200 µm;
– particle densities were 3.36 (Al_3Ti) and 4.95 g/cm^3 (TiC);
– shape of particles was characterized by flow drag coefficient.

The value of this parameter was 0.47 for spheroidal particle and 1.2 for plate-like particles [17].

In laboratory experiment, a charge consisting of aluminium-TiC composite scrap was used. It was melted in an electric induction furnace in a clay-graphite crucible. The aluminium composite had been synthetised previously via the SHS-B method, with the volume fraction of TiC in the composite being approximately 10%. Melting and casting of the composite were carried out in air atmosphere. Following remelting and overheating to 800 °C , the composite was first poured gravitationally into a small iron mould. Subsequently the molten composite suspension was poured into a rotating mould with a vertical axis of rotation. The mould was prepared from furan sand, and its initial temperature was equal to ambient temperature. The sand mould was mounted within a steel cylindrical shell, and its rotational speed was set to 900 rpm.

The casted disc was cut in the two perpendicular planes, parallel to rotation axis. After the preparation of metal specimens by polishing, their microstructure was characterized using digital light microscope (LM) and scanning electron microscope (SEM) combined with energy-dispersive X-ray spectrometers (EDS). The volume fraction of reinforcement particles was examined in both the gravitationally cast, reference specimen, referred to as RS, and the centrifugally cast disc, referred to as CS, through the study. Chemical composition of obtained casting examined by SPECTROMAXx spark spectrometer is shown in table 1.

Table 1.
Chemical composition of aluminium-TiC composite, wt. %

Element	Si	Ti	Fe	Al
Contents	0.31	2.71	0.14	balance

The particle distribution and grain size were analysed in 15 fields taken from the outer, middle, and inner regions of the centrifugal casting. ImageJ software was used to quantify the particles volume fraction. Brinell hardness measurements were taken at various points along the radial section. A 5 mm diameter steel ball, a load of 613 N, and a dwell time of 30 s were used to characterise the hardness distribution.

3. Results

Centrifugal casting simulation is well-implemented in ProCAST software, particularly for conventional liquid alloys. However, simulating the flow of alloy mixtures containing ceramic particles remains challenging, especially when the aim is to examine the particle distribution. Based on the liquid metal flow simulation data, the post-processor implemented in ProCAST software, calculates the trajectories of the particles. We performed an analysis of the influence of particle density, size, and shape on its movement and final distribution.

The results presented in Fig. 1 show that the liquid alloy gradually fills the mould from the outer surface towards the centre. It is visible that the liquid alloy together with the particles flows along the lower surface of the mould cavity. In Fig. 2 (a-b) the particle trajectories are shown. The red and blue lines represent the trajectory along which particles with densities of 3.36 and 4.95 g/cm^3 flow. The simulation results show that denser particles are distributed closer to the outer surface of the casting.

a) b)

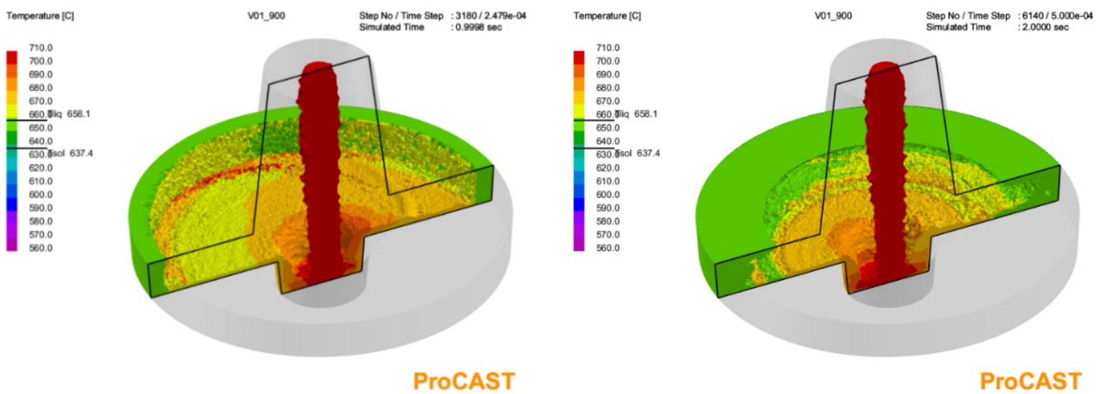

Fig. 1. Simulation results at 1s (a) and 2 s (b) following the initiation of pouring

a) b)

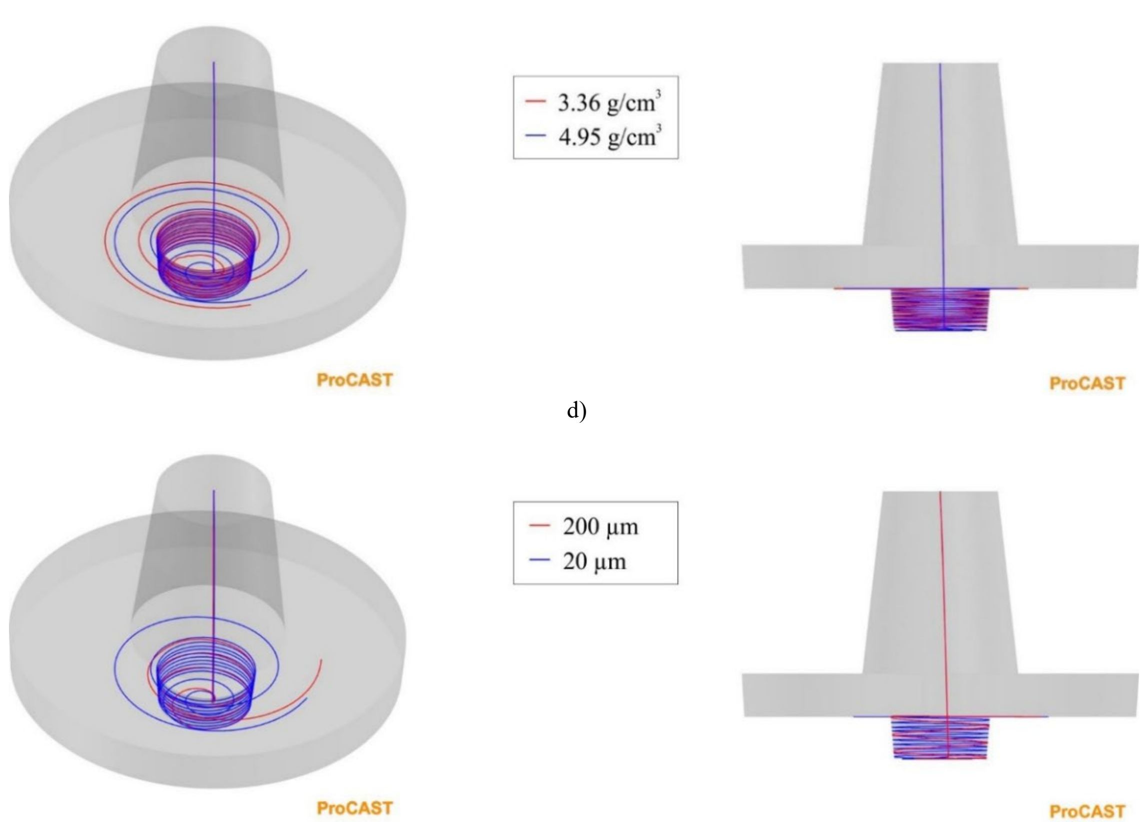

Fig. 2. Simulation results for particles with densities of 4.95 and 3.36 g/cm^3 and a diameter of 20µm (a, b) and for particles with diameters of 20 µm and 200 µm and a density of 4.95 g/cm^3 (c, d)

The influence of particle diameter on movement trajectory is presented in Fig. 2 (c-d). Particles with larger diameters move faster through liquid aluminium and migrate further from the axis of rotation, compared to those with diameters below 20 µm. As a result, larger particles travel greater distances than smaller ones. Fig. 2 (c-d) shows that particles with a diameter of 200 µm flow up from the sprue basin after four rotations, whereas particles with a diameter of 20 µm require more than ten rotations. The simulation results indicate that the position of the ceramic particles varies along the radius of the disc.

In the second part of our investigation, we carried out an experiment under laboratory conditions. The typical microstructure of the obtained AFGM is presented in Fig. 3. The microstructure consists of an aluminium matrix and two different types of particles. The finer particles, are located at the grain boundaries, while the plate-like particles, are particularly visible near the outer surface of the centrifugal casting (Fig. 3b). SEM analysis revealed that the interdendritic particles are rich in titanium and carbon, whereas the plate-like particles are rich in titanium and aluminium.

Furthermore, during solidification, the TiC particles are repelled by the solid phase and exhibit strong pinning effect, which inhibits the growth of aluminium dendrites. Consequently, the average grain size of α-Al is 50 µm in the outer zone and 93 µm in the inner zone

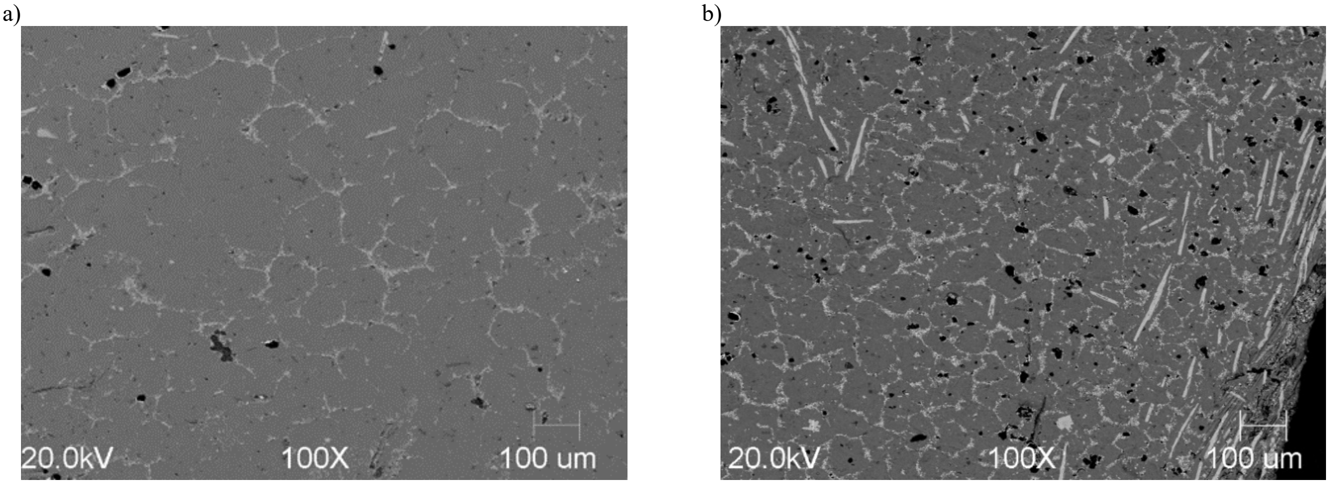

Fig. 3. SEM (BSE) microstructure of the inner (a) and outer (b) regions of the centrifugal casting. The rotation axis is located on the left side of the images

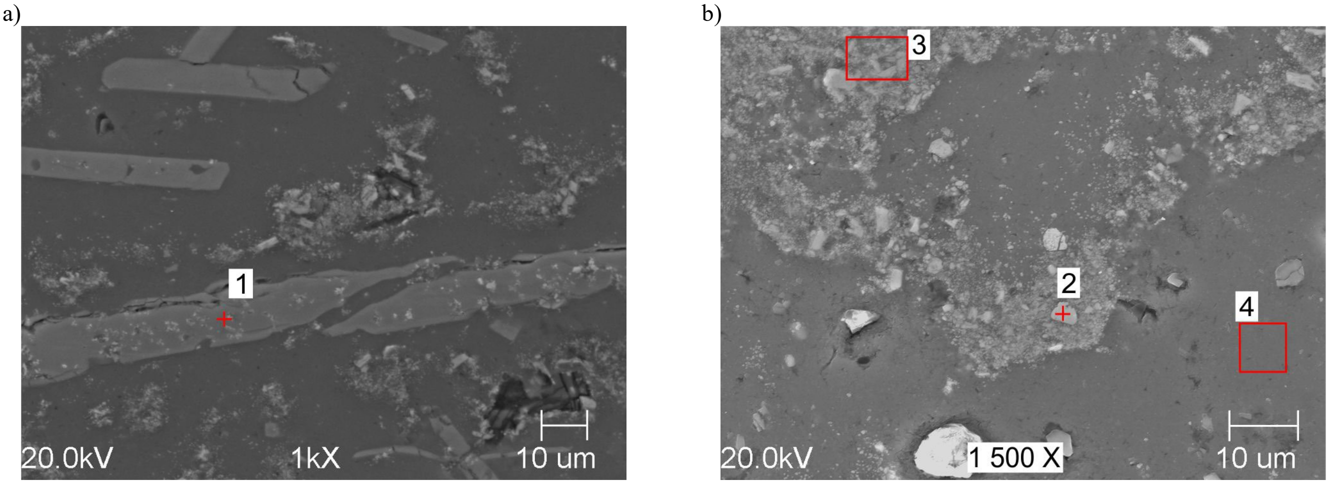

Fig. 4. Microstructure of phases observed in the outer region of the centrifugal casting

SEM images of the particles observed in the microstructure of the examined AFGM are presented in Fig. 4. In the outer area of the casting, Al_3Ti particles are primarily observed (Fig. 4a), whereas in the interdendritic areas, fine titanium carbide particles are the dominant phase (Fig. 4 b). The results of the EDS analysis of this phases are presented in Table 2. The relatively high overheating temperature during melting, influenced the thermal decomposition of TiC into Al_3Ti and Al_4C_3. Both phases are observed in the microstructure (See Figs. 4a and 5). In the outer region of the microstructure, Al_3Ti plates are visibly aligned nearly parallel to the vertical mould surface. This suggests that the plate-like particles migrate through the liquid phase towards the outer surface, where their movement is likely impeded by a formation of a solid layer. In contrast, the finer titanium carbide particles moved more slowly and, during solidification, are repelled by the growing dendrite arms of the solid phase. As a result, these particles are distributed within the interdendritic regions of the α-Al matrix.

Table 2.
EDS analysis of the phases shown in Figs. 4 and 5, mass %

Element	Spot 1	Spot 2	Area 3	Area 4	Spot 5	Spot 6
C	-	9.510	17.552	0.564	28.602	30.224
O	-	22.701	0.862	0.177	0.035	1.938
Al	63.138	64.362	42.928	98.795	40.975	67.408
Si	0.172	0.031	0.146	0.025	0.267	0.078
Ti	24.539	3.229	36.717	0.351	30.033	0.331
Fe	0.120	0.166	1.795	0.087	0.088	0.022

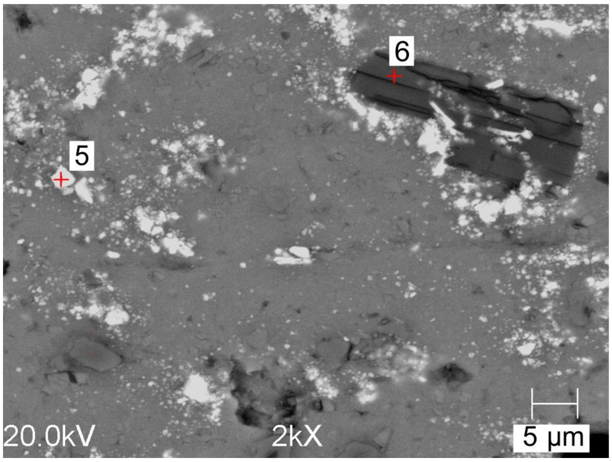

Fig. 5. Microstructure of titanium and aluminium carbides observed in casting

Changes in volume fraction and hardness through the cross section of the examined disc are shown in Fig. 6. In the RS, the volume fraction of the particles was 9.9 wt.%, as indicated by the dashed line in Fig. 6a. It is clear that the volume fraction of particles is higher in the outer region than in the inner region of CS. The volume fraction at a distance of 30 mm from the rotation axis was 6%, increasing to 12% at a distance of 65 mm. This demonstrates that the centrifugal force promotes the segregation of particles towards the outer surface of the casting. Larger plate-like Al_3Ti particles are visible near the outer surface despite their lower density compared to TiC (the density of Al_3Ti is 3.36 g/cm^3, [18] whereas that of TiC is 4.95 g/cm^3).

This phenomenon can be explained using Stokes' law. According to this law and considering the forces acting on the particle (buoyant, and centrifugal), the velocity of a particle moving through a liquid can be expressed by the following equation: [3]

$$v_p = \frac{(\rho_p - \rho_l)\omega^2 \cdot r \cdot D_p^2}{18\mu} \quad (1)$$

where $\rho_{p,l}$ is density of particles and liquid, ω - angular velocity, r - is distance from the axis of rotation, D_p - is particle diameter, μ is viscosity of liquid alloy.

According to (1), the velocity of particles moving through a liquid is directly proportional to the density difference between the particle and the fluid, the particle radius, and the angular velocity, and inversely proportional to the dynamic viscosity of the liquid. When density, viscosity, and angular velocity are constant, the variable influencing particle velocity is their radius. Based on (1) the velocity of particles can be calculated. It is evident that particles with a diameter of 1 µm, for example, move at a higher velocity than those with a diameter of 10 µm. This calculation results align with the observed particle distribution in microstructure of CS.

The results of hardness measurements are presented in Fig. 6b. In the inner region of the CS, the hardness is 23 HB and increases towards the outer region, reaching 28 HB. These hardness values correlate with the volume fraction of reinforcing particles in the casting. Generally, the increase in hardness is influenced by the higher volume fraction of TiC and Al_3Ti particles. However, detailed microstructural observations reveal that the grains in the outer region are finer than those in the inner region (see Figs. 3a and 3b). This visible grain refinement in the outer region is induced by the pinning effect of fine TiC particles, which accumulate on the solidification front and impede dendrite growth, thereby affecting the AFGM hardness.

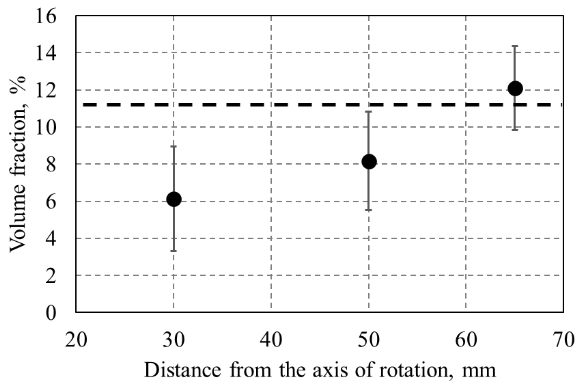

a)

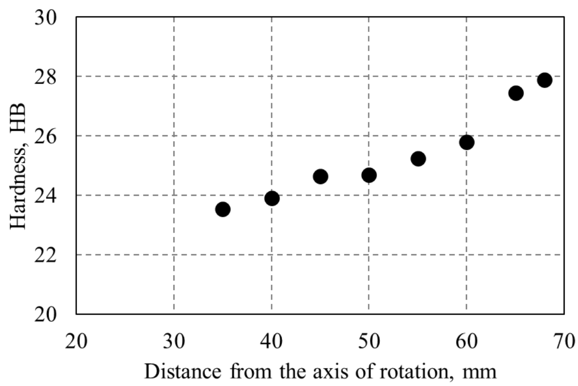

b)

Fig. 6. Volume fraction of particles (a) and the hardness (b) in the cross-section of the disc

4. Conclusions

1. The simulation results showed that liquid alloy and particles move along the lower surface of the mould cavity during the centrifugal casting process.
2. Under centrifugal force, the larger, lower-density particles moved more rapidly through the molten aluminium.
3. An increased volume fraction of TiC/Al_3Ti particles in the outer region resulted in a higher Brinell hardness.
4. The refinement of aluminium dendrites was influenced by the presence of fine TiC particles.
5. Large Al_3Ti phase plates are predominantly located near the outer surface of the casting, with their orientation being nearly parallel to the surface.
6. The rotation speed and pouring temperature were insufficient to achieve a composite zone with a high particle density in the outer region of the casting.

Acknowledgements

Financial support of the National Science Centre (NCN), Poland (project no. 2021/43/B/ST8/03271) is greatly acknowledged.

References

[1] Reichardt, A., Shapiro, A.A., Otis, R., Dillon, R.P., Borgonia, J.P., McEnerney, B.W., Hosemann, P. & Beese, A.M. (2021). Advances in additive manufacturing of metal-based functionally graded materials. *International Materials Reviews.* 66(1), 1-29. DOI: 10.1080/09506608.2019.1709354.

[2] Charan, M.S., Naik, A.K., Kota, N., Laha, T. & Roy, S. (2022). Review on developments of bulk functionally graded composite materials. *International Materials Reviews.* 67(8), 797-863. DOI: 10.1080/09506608.2022.2026863.

[3] Ogawa, T., Watanabe, Y., Sato, H., Kim I.S. & Fukui, Y. (2006). Theoretical study on fabrication of functionally graded material with density gradient by a centrifugal solid-particle method. *Composites Part A: Applied Science and Manufacturing.* 37(12), 2194-2200. DOI: 10.1016/J.COMPOSITESA.2005.10. 002.

[4] Heidary, D.S.B. & Akhlaghi, F. (2011). Theoretical and experimental study on settling of SiC particles in composite slurries of aluminum A356/SiC. *Acta Materialia.* 59(11), 4556-4568. https://doi.org/10.1016/J.ACTAMAT.2011.03.077.

[5] Verma, R.K., Parganiha, D. & Chopkar, M. (2021). A review on fabrication and characteristics of functionally graded aluminum matrix composites fabricated by centrifugal casting method. *SN Applied Science*. 3(2), 1-29 DOI: /10.1007/s42452-021-04200-8

[6] Jackowski, J. & Szymański, P. (2012). The structure of centrifugally cast composite casting. *Composites theory and practice.* 12(1), 66-71.

[7] Dolata-Grosz, A., Śleziona, J., Wieczorek, J. & Dyzia, M. (2002). Layered structure of AK12-Al2O3 and AK12- SiC composites formed by the centrifugal casting. *KOMPOZYTY (COMPOSITES).* 5, 305-308.

[8] Wang, K., Zhang, Z.M., Yu, T., He, N.J. & Zhu, Z.Z. (2017). The transfer behavior in centrifugal casting of SiCp/Al composites. *Journal of Materials Processing Technology*. 242, 60-67. DOI: 10.1016/j.jmatprotec.2016.11.019. https://doi.org/10.1016/j.jmatprotec.2016.11.019.

[9] Tęcza, G. (2012). Changes in abrasive wear resistance during miller test of Cr-Ni cast steel with Ti carbides formed in the alloy matrix. *Archives of Foundry Engineering.* 21(4), 110-115. DOI: 10.24425/afe.2021.139758.

[10] Maziarz, W., Wójcik, A., Chulist, R., Bigos, A., Kurtyka, P., Szymański, Ł., Jimenez Zabaleta, A., García de Cortázar, M. & Olejnik, E.(2024). Microstructure and mechanical properties of Al/TiC and Al/(Ti,W)C nanocomposites fabricated via in situ casting method. *Journal of Materials Research and Technology.* 28, 1852-1863. DOI: 10.1016/j.jmrt.2023.12.126.

[11] Sobula, S., Olejnik, E. & Tokarski, T. (2017). Wear resistance of TiC reinforced cast steel matrix composite. *Archives of Foundry Engineering*. 17(1), 143-146. DOI: 10.1515/afe-2017-0026.

[12] Maziarz, W., Wójcik, A., Bobrowski, P., Bigos, A., Szymański, Ł., Kurtyka, P., Rylko, N. & Olejnik, E. (2019). SEM and TEM studies on in-situ cast Al-TiC composites. *Materials Transactions*. 60(5), 714-717. DOI: 10.2320/matertrans.MC 201806

[13] David Raja Selvam, J., Dinaharan, I., Rai, R.S. & Mashinini, P.M. (2019). Dry sliding wear behaviour of in-situ fabricated TiC particulate reinforced AA6061 aluminium alloy. *Tribology-Materials, Surfaces & Interfaces.* 13(1), 1-11. DOI: 10.1080/17515831.2018.1550971.

[14] Kennedy, A.R., Weston, D.P. & Jones, M.I. (2001). Reaction in Al–TiC metal matrix composites. *Materials Science and Engineering A.* 316(1-2), 32-38. DOI: 10.1016/S0921-5093(01)01228-X.

[15] Verma, R.K., Biswas, P. & Chopkar, M.K. (2023). Simulation and experimental investigation of centrifugal-cast functionally graded aluminum-B4C composite. *Materials and Manufacturing Processes.* 38(13), 1729-1743. DOI: 10.1080/ 10426914.2023.2176879.

[16] Dolata, A.J., Golak, S. & Ciepliński, P. (2017). The Eulerian multiphase model of centrifugal casting process of particle reinforced Al matrix composites. *Composites. Theory and Practice*. 17(4), 200-205.

[17] Nakayama, Y. (2018). *Introduction to Fluid Mechanics (2-nd Edition). Elsevier*. Retrieved July 7, 2025, from https://app.knovel.com/hotlink/pdf/id:kt011PH782/introduction-fluid-mechanics/beginning-fluid-mechanics. ISBN: 978-0-08-102437-9.

[18] Nakamura, M. & Kimura, K. (1991). Elastic constants of $TiAl_3$ and $ZrAl_3$ single crystals. *Journal of Materials Science*, 26(8), 2208-2214. DOI: 10.1007/BF00549190.